Article

Discovery Medicine 2024; 36(180): 190–198
https://doi.org/10.24976/Discov.Med.202436180.18

Effect of Cichoric Acid on Colorectal Cancer: Impact on Migration, Epithelial-Mesenchymal Transition, and Proliferation *via* RhoA/ROCK Signaling Pathway Modulation

Sheng Ma[1,†], Zaiyu Huang[1,†], Qifeng Chen[2,*], Xuewen Yin[3,*]

[1]Department of Anorectal, Xianning Central Hospital, The First Affiliated Hospital of Hubei University of Science and Technology, 437100 Xianning, Hubei, China
[2]Department of Nursing, Xianning Hospital of Traditional Chinese Medicine, 437100 Xianning, Hubei, China
[3]Department of Surgery, Jiayu Hospital of Traditional Chinese Medicine, 437200 Xianning, Hubei, China
*Correspondence: 15872835007@163.com (Qifeng Chen); yxuewen87@163.com (Xuewen Yin)
[†]These authors contributed equally.
Published: 20 January 2024

Background: Colorectal cancer (CRC) is a common malignancy with high morbidity and mortality. To improve CMC prognosis, research must identify safe and effective natural drugs that improve the proliferation, migration, and epithelial mesenchymal transition (EMT) processes of CRC. The purpose of this paper is to understand how cichoric acid (CA) impacts CRC proliferation, metastasis, and EMT of CRC by adjusting the Ras homolog family member A (RhoA)/RHO-associated coiled coil protein kinase (ROCK) pathway.

Methods: Human Colon Cancer Cells (HCT116) cells were randomly divided into Control (blank medium treatment), low concentration CA (CA-L), medium concentration CA (CA-M), high concentration CA (CA-H), and high-concentration CA+RhoA activator U46619 (CA-H+U46619) groups. Cell proliferation, migration and invasion, and apoptosis were evaluated with cell counting kit-8 (CCK-8) assay, transwell assay, and flow cytometry, respectively. The expression of RhoA, ROCK, and EMT-associated proteins were detected by Western Blot. The CRC transplanted tumor model of nude mice was constructed, and the mice were grouped into low-dose CA (CA-Low, 15 mg/kg CA), high-dose CA (CA-High, 30 mg/kg CA), high-dose CA+RhoA activator U46619 (CA-High+U46619, 30 mg/kg CA+10 mM U46619), and Model groups at random, with 12 mice in each group. Tumor volume, mass, and inhibition rate were measured and calculated, and the pathological changes of tumor in nude mice were detected by hematoxylin-eosin (HE) staining.

Results: Compared with Control, the optical density of cells at 450 nm (OD_{450}) value (48 h, 72 h), cell migration number, cell invasion number, RhoA, ROCK1, N-cadherin, vimentin protein expression levels of HCT116 cells were reduced in CA-M and CA-H groups; however, E-cadherin level and apoptosis rate were increased ($p < 0.05$). In the CA-High group, we observed a significant decrease ($p < 0.05$) in both tumor volume and mass in nude mice. Additionally, the tumor tissue cells exhibited better organization, reduced size, reduced tumor and vascular tissue hyperplasia, and decreased infiltration of inflammatory cells. U46619 decreased the retardation of CA on the proliferation, EMT, and migration of CRC tumor cells as well as the growth of transplanted CRC tumors in nude mice.

Conclusions: CA may reduce CRC migration, proliferation, and EMT by inhibiting the activation of the RhoA/ROCK signaling pathway.

Keywords: cichoric acid; Ras homolog family member A; Rho associated coiled coil protein kinase; colorectal cancer; migration; epithelial-mesenchymal transition

Introduction

Colorectal cancer (CRC) is a common malignant tumor with a high morbidity and mortality. Based on the latest global cancer burden data, CRC ranks second in new tumor cases in China, and the fifth in cancer-related patient mortality [1]. The current clinical treatment for CRC is radical resection, but patient cure and survival rates remain insignificant, possibly due to distant tumor metastasis as a result of middle and late-stage diagnosis [2,3]. Among CRC patients, it is expected that about 60% will experience metastasis. Of note, tumor metastasis is closely related to the process of epithelial mesenchymal transition (EMT) [4]. Thus, finding safe and effective natural drugs to inhibit the proliferation, migration, and EMT process of CRC can help enhance the survival rate of CRC patients.

Cichoric acid (CA) is a caffeic acid component extracted and separated from chicory in the composite family. Modern pharmacological studies have found that CA has anti-inflammatory, antioxidant, antiviral, anticancer, immune enhancement, and other pharmacological effects [5,6]. In recent years, relevant literature has shown that CA inhibits cancer progression and tumor growth by inducing autophagy and cell apoptosis, particularly in gastric cancer cells [7]. However, there is currently limited research on CA in colorectal cancer.

Ras homolog gene family member A (RhoA)/Rho-associated coiled coil protein kinase (ROCK) pathway is closely related to tumor metastasis, and activated RhoA can activate downstream factor ROCK1 to promote cell metastasis [8,9]. The purpose of this study was to construct a nude mouse CRC transplant tumor model and culture human CRC cell line Human Colon Cancer Cells (HCT116), and to discuss the specific mechanisms of CA affecting CRC proliferation, migration, and EMT.

Materials and Methods

Cells

HCT116 cells were obtained by the stem cell bank of the Chinese Academy of Sciences (NM-J03, Shanghai, China) and acquired cells were tested for mycoplasma and short tandem repeat (STR) identified.

Experimental Animals

Forty-eight Balb/c-nu nude mice, male, weighing 18–22 g, were provided by Zhongyan Zichuang (Beijing) Biotechnology Co., Ltd. (Beijing, China), animal license number: SCXK (Beijing) 2022-0010. The nude mice were kept in SPF (specific pathogen free) surroundings. The drinking water and food were sterilized and kept in cages with 12 hours of light/darkness per day. The animal experiment scheme was reviewed and ratified by the ethics committee of Xianning Central Hospital (reference number: XNCH2022035).

Main Reagents and Instruments

Cichoric acid was obtained by Shanghai Yuanye Biotechnology Co., Ltd. (B20647, 324895, Shanghai, China); Roswell Park Memorial Institute (RPMI)-1640 was provided by HyClone (247536, Logan, UT, USA); transwell cubicle provided by Corning (152689, Corning, NY, USA); cell counting kit-8 (CCK-8) kit was provided by Shanghai Biyuntian Company (336025, Shanghai, China); hematoxylin-eosin (HE) staining kit and apoptosis detection kit were provided by Beijing Solaibao Technology Co. (502189, 568247, Beijing, China). Anti-RhoA, anti-ROCK1, E-cadherin, N-cadherin, Vimentin, glyceraldehyde-3-phosphate dehydrogenase (GAPDH), and sheep anti-rabbit IgG secondary antibodies were provided by Abcam (CAS#26807-65-8, CAS#1415565-02-4, 924420, 569240, CAS#156289-80-4, CAS#9001-50-7, 358214, Cambridge, UK). Enzymoleter was provided by Thermo Fisher (Multiskan SkyHigh, New York, NY, USA). Optical microscope was provided by Shanghai Guangmi Instrument Co., Ltd. (GMM900, Shanghai, China). Flow cytometry was provided by Thermo Fisher (Attune CytPix, New York, NY, USA). The flow cytometry software used in this study was Flow Jo (version 10, BD Biosciences, New York, NY, USA).

Cell Culture

HCT116 cells were put into RPMI-1640 medium containing 10% fetal bovine serum. The cell state was closely monitored, ensuring timely fluid changes and initiating cell passage when the cell fusion reached around 90%. After three passages, cells in the logarithmic stage were selected for subsequent experiments.

Cell Grouping and Treatment

The logarithmic HCT116 cells were randomly divided into low concentration CA (CA-L, 50 μg/mL CA), medium concentration CA (CA-M, 100 μg/mL CA), high concentration CA (CA-H, 200 μg/mL CA [10]), high-concentration CA+RhoA activator U46619 (CA-H+U46619, 200 μg/mL CA+10 nM U46619 [11]) and Control (blank medium treatment) groups.

Cell Proliferation Assay

The logarithmic HCT116 cells were categorized and subjected to treatment following the specified concentration parameters. These cells were then cultured in 96-well cell plates. Each well was supplemented with 10 μL CCK-8 reagent at 24, 48, and 72 h. After 2 h incubation, an enzymoleter was used to measure the optical density of cells at 450 nm (OD_{450}).

Cell Migration Assay

RPMI-1640 medium was added to the lower chamber of the transwell, while the upper chamber received a suspension of HCT116 cells. The cells were fixed with paraformaldehyde and stained with crystal violet after 48 h. The positive cells, which appear purple, were viewed under a microscope, then photographed and counted.

Cell Invasion Assay

The Matrigel matrix glue was diluted with serum-free medium and applied to the upper compartment membrane of the transwell. It was then placed at 37 °C for 4 h to solidify. For other steps, see “Cell migration Assay”.

Apoptosis Analysis

Logarithmic HCT116 cells were collected after treatment according to the operation in “Cell Grouping and Treatment” and washed twice with PBS. Afterwards, the

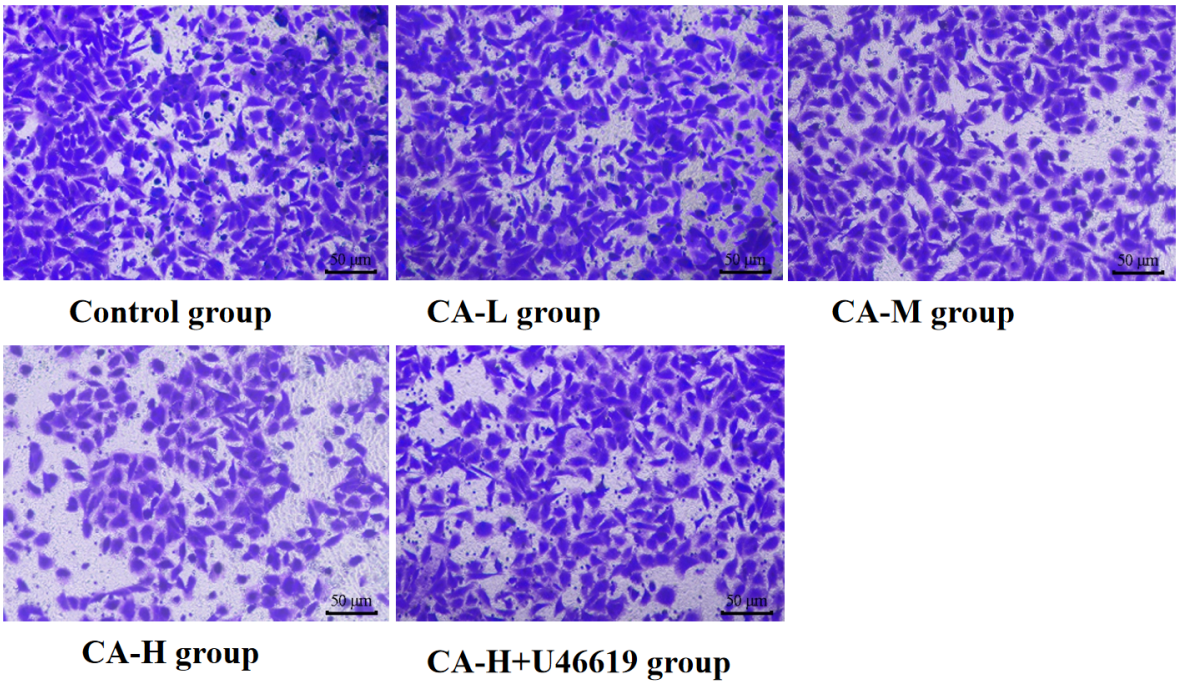

Fig. 1. Migration of HCT116 cells was detected by transwell method (crystal violet staining). The scale bar was 50 μm.

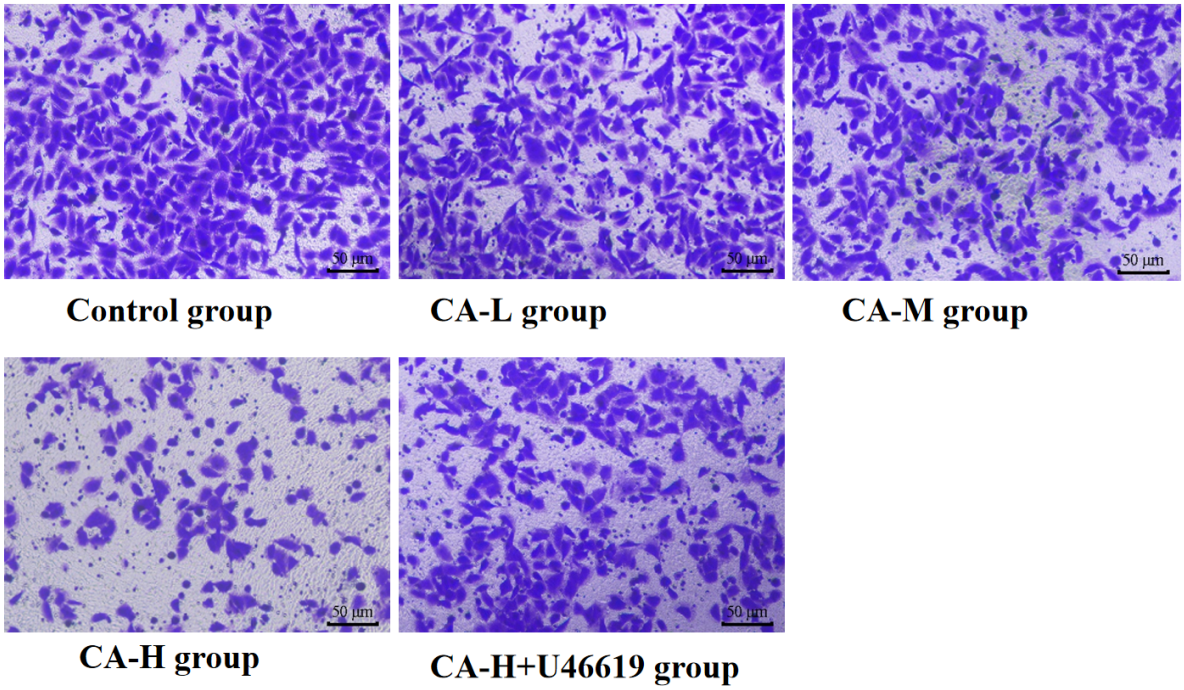

Fig. 2. Transwell method was used to measure invasion of HCT116 cells (crystal violet staining). The scale bar was 50 μm.

HCT116 cells were thoroughly mixed and subsequently incubated without light with 500 μL of binding buffer, 10 μL PI, and 5 μL AnnexinV-FITC. Flow cytometry was performed to assess apoptosis.

Western Blot Analysis

After treatment of "Cell Grouping and Treatment", HCT116 cells were collected and the total protein of the cells was extracted. The protein was quantified and subsequently subjected to SDS-PAGE, membrane transfer, and sealed for 1 h. RhoA, ROCK1, E-cadherin, N-cadherin, Vimentin, and GAPDH (all 1:1000) were added and left to incubate overnight at 4 °C. The following day, corresponding secondary antibodies (1:5000 dilution) were applied and incubated for 2 h with ECL reagent (36208ES60, Yisheng Biotechnology Co., Ltd., Shanghai, China) for color devel-

Table 1. Comparison of the proliferative activity of HCT116 cells ($\bar{x} \pm s$, n = 6).

Group	OD_{450} value		
	24 h	48 h	72 h
Control	0.17 ± 0.02	0.58 ± 0.06	0.88 ± 0.09
CA-L	0.16 ± 0.02	0.56 ± 0.06	0.83 ± 0.08
CA-M	0.18 ± 0.05	0.34 ± 0.03*#	0.60 ± 0.06*#
CA-H	0.16 ± 0.04	0.21 ± 0.02*#&	0.32 ± 0.03*#&
CA-H+U46619	0.17 ± 0.05	0.49 ± 0.05^	0.72 ± 0.07^

Note: *$p < 0.05$ vs Control group; #$p < 0.05$ vs CA-L group; &$p < 0.05$ vs CA-M group; ^$p < 0.05$ vs CA-H group. CA, cichoric acid; CA-L, low concentration CA; CA-M, medium concentration CA; CA-H, high concentration CA; CA-H+U46619, high-concentration CA+RhoA activator U46619; HCT116, Human Colon Cancer Cells; OD_{450}, optical density of cells at 450 nm.

Table 2. Comparison of HCT116 cell migration numbers ($\bar{x} \pm s$, n = 5).

Group	Number of cell migrations
Control	187.22 ± 13.03
CA-L	182.59 ± 12.61
CA-M	145.26 ± 9.66*#
CA-H	103.18 ± 10.57*#&
CA-H+U46619	160.47 ± 12.39^

Note: *$p < 0.05$ vs Control group; #$p < 0.05$ vs CA-L group; &$p < 0.05$ vs CA-M group; ^$p < 0.05$ vs CA-H group.

opment. The protein bands were observed, and the relative expression of the target protein was analyzed using Image Lab™ software (version 3.0.39529, MCM DESIGN, Los Angeles, CA, USA).

Establishment of Transplanted Tumor Model in Nude Mice

HCT116 cells were routinely cultured and collected, and PBS was used to adjust the cell concentration to 1.8×10^7 cells/mL cell suspension. The HCT116 cell suspension was subcutaneously injected into the armpit of each nude mouse, with 0.1 mL inoculated per mouse. After about 6 days of inoculation, rice-like granular protrusions appeared at the inoculation site of nude mice and gradually increased in size, indicating the successful construction of a CRC tumor transplantation model in nude mice [4].

Grouping and Treatment of Nude Mice

48 nude mice who succeeded in modeling were randomly grouped into Model, low-dose CA (CA-Low, 15 mg/kg), high-dose CA (CA-High, 30 mg/kg [12]) and high-dose CA+RhoA activator U46619 (CA-High+U46619, 30 mg/kg CA+10 mM U46619 [13]) groups, with 12 mice in each group. The does was started once the transplanted tumor grew to 100 mm^3. CA was administered by intragastric administration and U46619 was administered intraperitoneally once daily for 3 weeks. In the Model group, mice received an equal amount of normal saline by gavage and intraperitoneal injection. Both the CA-Low and CA-High groups were given the same amount of normal saline daily through intraperitoneal injection.

Table 3. Comparison of HCT116 cell invasion numbers ($\bar{x} \pm s$, n = 5).

Group	Number of cell invasions
Control	169.57 ± 12.33
CA-L	162.45 ± 10.38
CA-M	124.28 ± 10.50*#
CA-H	77.63 ± 8.59*#&
CA-H+U46619	118.09 ± 13.26^

Note: *$p < 0.05$ vs Control group; #$p < 0.05$ vs CA-L group; &$p < 0.05$ vs CA-M group; ^$p < 0.05$ vs CA-H group.

Determination of Tumor Volume and Inhibition Rate

After the last administration, nude mice were anesthetized with sodium pentobarbital (45 mg/kg) and were euthanized through cervical dislocation and underwent aseptic surgery to remove tumor tissue. The long diameter (a) and short diameter (b) of tumors in each nude mouse were recorded and the average tumor weight was calculated for each group. Tumor inhibition rate (%) = $(m_{\text{model group}} - m_{\text{administration group}})/m_{\text{model group}} \times 100\%$. Tumor Volume ($mm^3$) = $ab^2/2$.

HE Staining Observation of Pathological Changes in Tumor Tissue

The tumor tissue of nude mice was removed and immediately fixed in paraformaldehyde. Subsequently, the tissue was dehydrated and embedded with paraffin to prepare pathological sections of tumor tissue for analysis. After HE staining, the pathological changes of tumor tissue were observed (×400).

Statistical Analysis

Graph Pad Prism 7.0 (GraphPad Software, Santiago, CA, USA) software was used to analyze the measurement data, which was expressed as mean ± standard deviation ($\bar{x} \pm s$). One-way ANOVA was performed to compare the differences among multiple groups, and LSD-*t* test was performed on further pairwise comparison. Statistical significance was established at $p < 0.05$.

Results

Effects of CA on Proliferation Activity

As expressed in Table 1, the OD_{450} value (48 h and 72 h) of HCT116 cells in CA-M, H groups was lower than those in Control group. The OD_{450} value (48 h, 72 h) of HCT116 cells decreased gradually with increasing CA

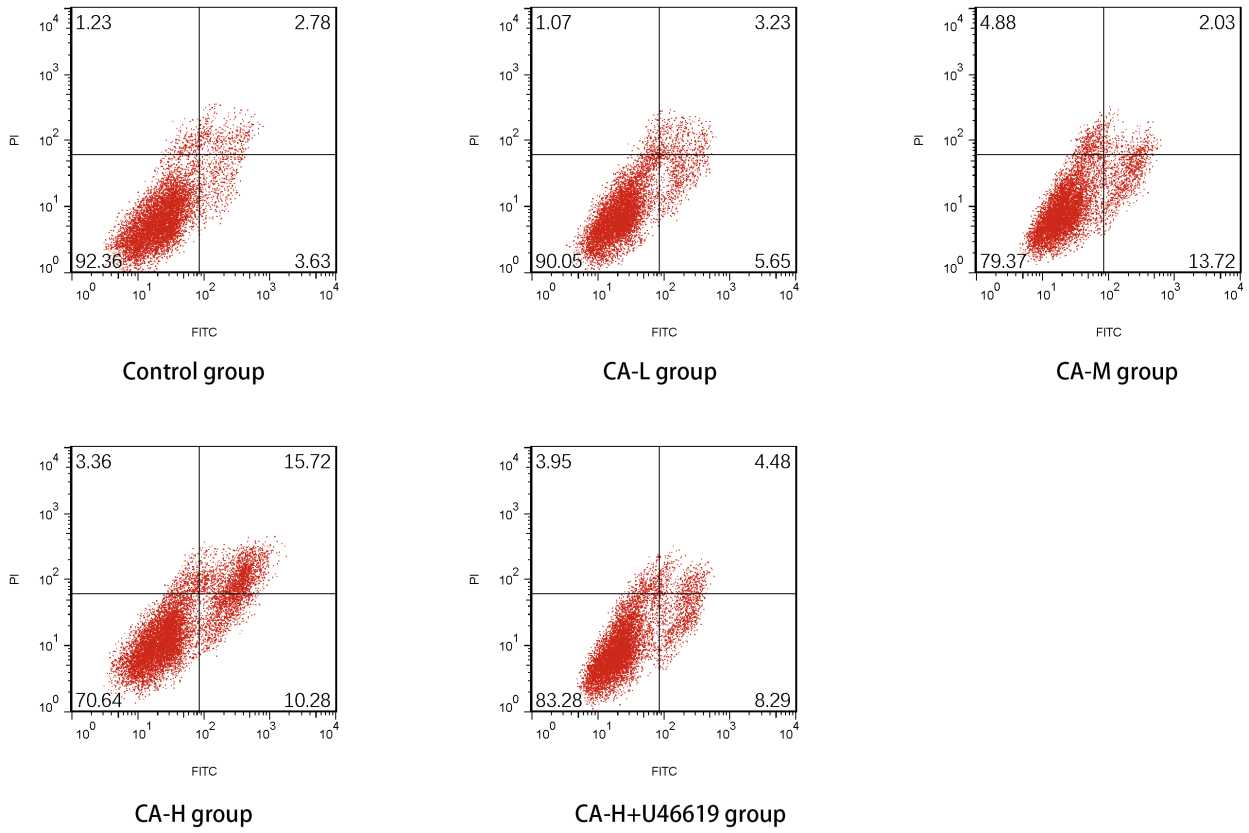

Fig. 3. Flow cytometry detection of apoptosis in HCT116 cells.

Table 4. Comparison of apoptosis rate of HCT116 cells ($\bar{x} \pm s$, n = 6).

Group	Apoptosis rate (%)
Control	6.46 ± 0.42
CA-L	8.55 ± 0.78
CA-M	15.43 ± 1.30*#
CA-H	26.15 ± 2.04*#&
CA-H+U46619	12.84 ± 1.49^

Note: *$p < 0.05$ vs Control group; #$p < 0.05$ vs CA-L group; &$p < 0.05$ vs CA-M group; ^$p < 0.05$ vs CA-H group.

dose. The OD_{450} value (48 h, 72 h) of HCT116 cells increased in CA-H+U46619 group compared with the CA-H group (all $p < 0.05$).

Effects of CA on Migration

In Table 2 and Fig. 1, the HCT116 cell migration was lower in CA-M and CA-H groups compared to Control group ($p < 0.05$) and HCT116 cell migration decreased gradually with increasing CA dose ($p < 0.05$). HCT116 cell migration increased in CA-H+U46619 group compared to the CA-H group ($p < 0.05$).

Effects of CA on Invasion

In Table 3 and Fig. 2, HCT116 cell invasion was reduced in the CA-M and CA-H groups compared to the Control group ($p < 0.05$). HCT116 cell invasion decreased gradually with increasing CA dose ($p < 0.05$). HCT116 cell invasion increased in the CA-H+U46619 group compared to the CA-H group ($p < 0.05$).

CA Affects Apoptosis

In Table 4 and Fig. 3, HCT116 cell apoptosis rate increased in the CA-M and CA-H groups compared with the Control group ($p < 0.05$). HCT116 cell apoptosis rate increased gradually with increasing CA dose ($p < 0.05$). Compared with the CA-L group, the apoptosis rate of both the CA-M and CA-H groups significantly increased ($p < 0.05$). Compared with the CA-M group, the cell apoptosis rate in the CA-H group significantly increased ($p < 0.05$). HCT116 cell apoptosis rate in the CA-H+U46619 group was significantly lower than those in the CA-H group ($p < 0.05$).

CA Affects the Expression of RhoA, ROCK, and EMT-Associated Proteins in HCT116 Cells

In Table 5 and Fig. 4, the levels of RhoA, ROCK1, N-cadherin, and Vimentin protein in HCT116 cells of the CA-M and CA-H groups were lower than those in the Con-

Table 5. Comparison of RhoA, ROCK, and EMT-associated proteins in HCT116 cells of each group ($\bar{x} \pm s$, n = 6).

Group	RhoA/GAPDH	ROCK1/GAPDH	E-cadherin/GAPDH	N-cadherin/GAPDH	Vimentin/GAPDH
Control	0.78 ± 0.08	0.85 ± 0.09	0.24 ± 0.02	0.89 ± 0.09	0.84 ± 0.08
CA-L	0.76 ± 0.08	0.83 ± 0.08	0.26 ± 0.03	0.87 ± 0.09	0.82 ± 0.08
CA-M	0.45 ± 0.05*#	0.60 ± 0.06*#	0.55 ± 0.06*#	0.66 ± 0.07*#	0.61 ± 0.06*#
CA-H	0.28 ± 0.03*#&	0.32 ± 0.03*#&	0.80 ± 0.08*#&	0.34 ± 0.03*#&	0.30 ± 0.03*#&
CA-H+U46619	0.56 ± 0.06^	0.65 ± 0.07^	0.48 ± 0.05^	0.63 ± 0.06^	0.58 ± 0.06^

Note: *$p < 0.05$ vs Control group; #$p < 0.05$ vs CA-L group; &$p < 0.05$ vs CA-M group; ^$p < 0.05$ vs CA-H group.

Table 6. Comparison of tumor volume, mass, and tumor inhibition rate of nude mice ($\bar{x} \pm s$, n = 12).

Group	Tumor volume (mm^3)	Tumor mass (mg)	Tumor inhibition rate (%)
Model	845.29 ± 125.37	1.27 ± 0.13	-
CA-Low	824.16 ± 119.70	1.14 ± 0.11	10.24
CA-High	374.54 ± 66.15*#	0.63 ± 0.05*#	50.39
CA-High+U46619	721.83 ± 94.33^	0.89 ± 0.09^	29.92

Note: *$p < 0.05$ vs Model group; #$p < 0.05$ vs CA-Low group; ^$p < 0.05$ vs CA-High group.

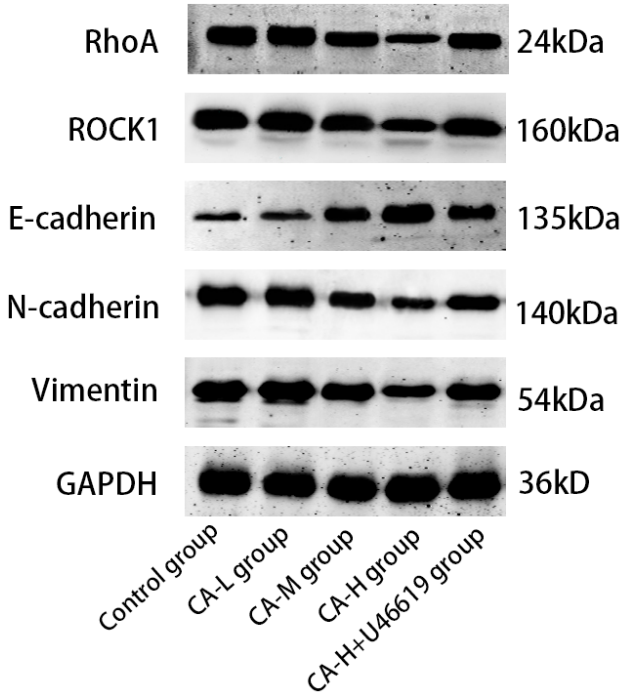

Fig. 4. Western Blot analysis of RhoA, ROCK, and EMT-associated proteins of HCT116 cells. RhoA, Ras homolog family member A; ROCK, RHO-associated coiled coil protein kinase; EMT, epithelial mesenchymal transition; GAPDH, glyceraldehyde-3-phosphate dehydrogenase.

trol group, while the expression of E-cadherin was higher. RhoA, ROCK1, N-cadherin, and Vimentin protein levels decreased gradually with increasing CA dose, however, the E-cadherin protein levels increased gradually, and all differences were statistically significant ($p < 0.05$). The levels of RhoA, ROCK1, Vimentin, and N-cadherin increased in the CA-H+U46619 group compared with the CA-H group, while E-cadherin expression was reduced (all $p < 0.05$).

Effects of CA on CRC Tumor Mass and Volume

As shown in Table 6, tumor volume and mass were reduced in the CA-H group compared with the Model group. The tumor volume and mass decreased in the CA-High group compared with the CA-Low group, however, the tumor inhibition rate increased. The tumor volume and mass increased in the CA-High+U46619 group compared with the CA-High group (all $p < 0.05$), however, the tumor inhibition rate decreased. Fig. 5 shows nude mice tumor photos from each group.

CA Affects Histopathological Changes of CRC Tumors

Fig. 6 illustrates that in the Model group, tumor cells exhibited a disorganized arrangement with larger cell volumes. Additionally, characteristics such as tumor tissue hyperplasia, vascular hyperplasia, and substantial infiltration of inflammatory cells were observed. The CA-Low group and CA-High group showed a more uniform arrangement of tumor tissue cells compared with the Model group. Additionally, these groups exhibited smaller cell volumes, reduced tumor tissue hyperplasia and vascular hyperplasia, and decreased infiltration of inflammatory cells. Notably, the pathological damage of tumor tissue in CA-High group was more evident, exceeding that of the CA-High+U46619 group.

Discussion

In China, there are up to 330,000 new CRC cases and 160,000 deaths every year, and the morbidity and mortality rate remain high [14]. The prognosis following radical CRC surgery is poor, with approximately 50% of patients dying due to tumor recurrence and metastasis within two years after surgery [15]. The pathogenesis and pathogenic factors of CRC are relatively complex, and researchers mainly believe that it is related to the interaction of genetics, envi-

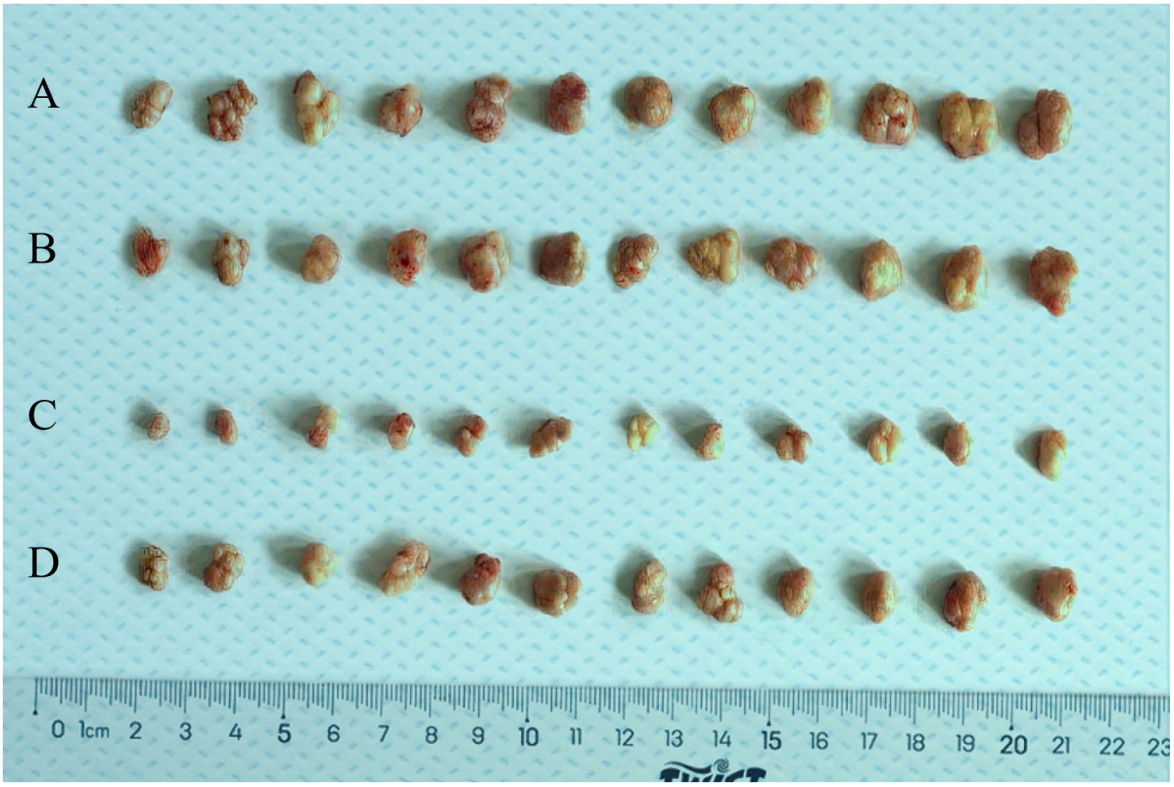

Fig. 5. Tumor photos of nude mice in each group. (A) Model group. (B) CA-Low group. (C) CA-High group. (D) CA-High+U46619 group.

ronment, diet, lifestyle, and other factors [16]. At present, the clinical treatment methods available for CRC offer limited efficacy. Surgical interventions are constrained by tumor staging, while chemotherapy often leads to significant side effects. Despite these treatments, tumor recurrence remains a major contributing factor to the high mortality rates among patients [17]. The process by which epithelial cells are transformed into mesenchymal phenotype through a specific program is called EMT, which is closely related to tumor metastasis [18]. Therefore, there is a clear need for safe and effective natural drugs that improve the therapeutic effect of CRC treatments.

CA is a kind of phenylpropionic acid compound widely existing in Compositae. More and more studies have proved that CA has good anti-tumor effect. Sun *et al.* [19] found that CA may induce autophagy and endoplasmic reticulum stress response through activation of adenosine 5′-monophosphate-activated protein kinase (AMPK) pathway, thus hindering the progression of cancer. CA can inhibit the growth of colon cancer tumor cells, which may be caused by reducing telomerase activity and inducing apoptosis [10]. The results of this study showed that CA can retard CRC cell proliferation, metastasis, and EMT, and induce their apoptosis *in vitro*. In addition, high-dose CA reduced tumor volume and mass in nude mice, mitigating pathological changes within CRC tumors. These results suggest that CA can inhibit CRC tumor growth *in vivo*.

The RhoA/ROCK signaling pathway is associated with the dynamic formation and decomposition of actin structures involved in tumor metastasis and invasion [20]. RhoA can participate in the invasion, proliferation, and other tumor processes, while ROCK1, as a downstream factor of RhoA, can enhance the phosphorylation of myosin, promote cell contractility, and promote tumor cell proliferation [21,22]. Ghasemi *et al.* [23] found that the RhoA/ROCK pathway can participate in the expression of leptin-induced UPA, thus promoting the invasion of leptin-induced ovarian cancer cells. Yang *et al.* [24] showed that the Numb protein can accelerate late-stage apoptosis in colon cancer while simultaneously inhibiting cell proliferation and tumor cell migration by inhibiting the RhoA/ROCK signaling pathway. In the present study, the levels of RhoA and ROCK1 in HCT116 cells within the CA-M and CA-H groups decreased, illustrating a potential connection between the anti-CRC effect of CA and the down-regulation of the RhoA/ROCK signaling pathway. We also established the CA-H+U46619 group, identifying that U46619 weakened the effect of CA on the proliferation, migration, and EMT of CRC tumor cells; moreover, the U46619 was able to delay tumor growth in nude mice.

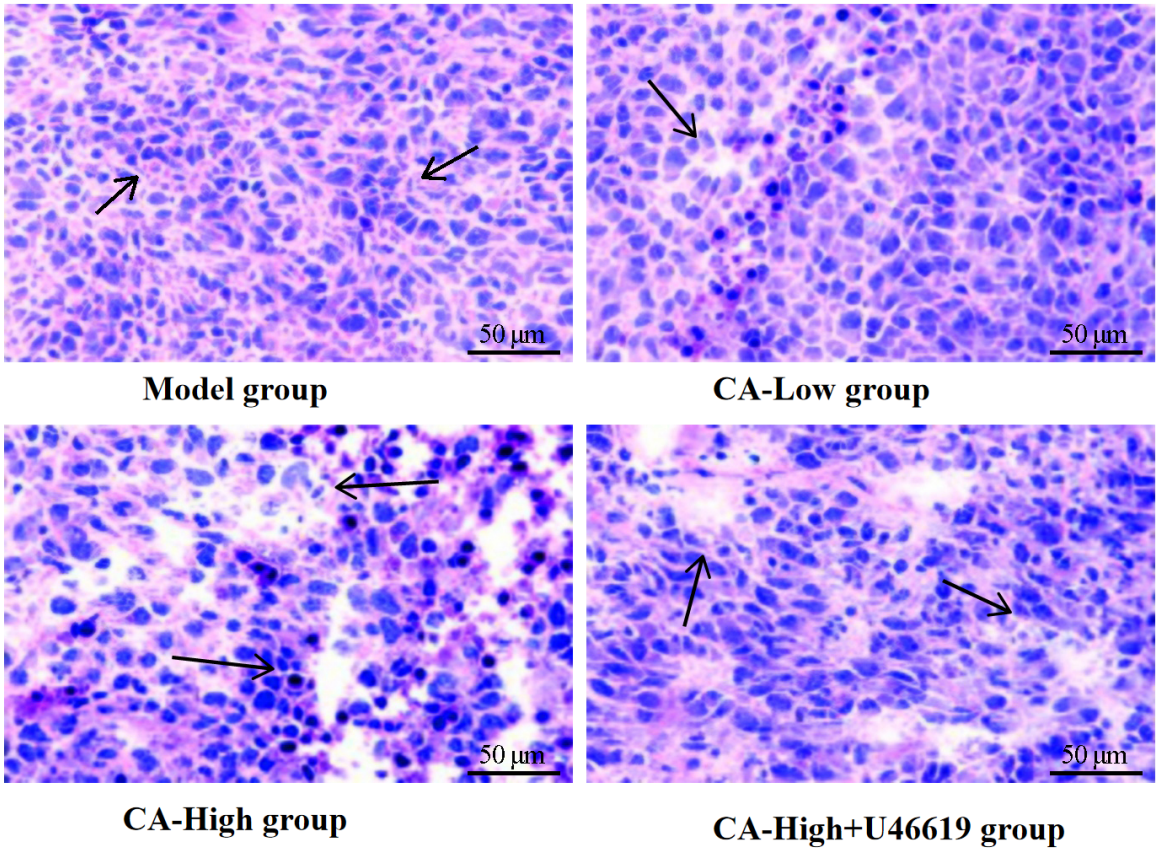

Fig. 6. Histopathological changes of colorectal cancer (CRC) tumor in nude mice observed by hematoxylin-eosin (HE) staining. The scale bar was 50 μm, the black arrow indicated the site of tumor tissue damage.

Conclusions

In conclusion, CA may retard the migration, proliferation, and EMT of CRC by down-regulating the RhoA/ROCK signaling pathway, which provides a scientific basis for the clinical development of novel drugs for CRC treatment. However, whether the inhibitory effect of CA on CRC tumor growth is related to other signaling pathways still needs to be further explored.

Availability of Data and Materials

The datasets used and/or analyzed during the present study are available from the corresponding authors on reasonable request.

Author Contributions

SM and ZH designed the research study. SM and ZH performed the research. XY and QC provided help and advice on the experiments. XY and QC analyzed the data. All authors contributed to editorial changes in the manuscript. All authors read and approved the final manuscript. All authors have participated sufficiently in the work and agreed to be accountable for all aspects of the work.

Ethics Approval and Consent to Participate

This study has been approved by the animal ethics committee of Xianning Central Hospital (XNCH2022035).

Acknowledgment

We would like to express our gratitude to the participants who generously gave their time and effort to make this study possible.

Funding

This research received no external funding.

Conflict of Interest

The authors declare no conflict of interest.

References

[1] Sung H, Ferlay J, Siegel RL, Laversanne M, Soerjomataram I, Jemal A, *et al*. Global Cancer Statistics 2020: GLOBOCAN Estimates of Incidence and Mortality Worldwide for 36 Cancers in 185 Countries. CA: a Cancer Journal for Clinicians. 2021; 71: 209–249.

[2] Raskov H, Søby JH, Troelsen J, Bojesen RD, Gögenur I. Driver

Gene Mutations and Epigenetics in Colorectal Cancer. Annals of Surgery. 2020; 271: 75–85.

[3] Patel SG, Karlitz JJ, Yen T, Lieu CH, Boland CR. The rising tide of early-onset colorectal cancer: a comprehensive review of epidemiology, clinical features, biology, risk factors, prevention, and early detection. The Lancet. Gastroenterology & Hepatology. 2022; 7: 262–274.

[4] Tang Q, Chen J, Di Z, Yuan W, Zhou Z, Liu Z, *et al*. TM4SF1 promotes EMT and cancer stemness via the Wnt/β-catenin/SOX2 pathway in colorectal cancer. Journal of Experimental & Clinical Cancer Research: CR. 2020; 39: 232.

[5] Lai TW, Cheng HL, Su TR, Yang JJ, Su CC. Cichoric Acid May Play a Role in Protecting Hair Cells from Ototoxic Drugs. International Journal of Molecular Sciences. 2022; 23: 6701.

[6] Luo Z, Gao G, Ma Z, Liu Q, Gao X, Tang X, *et al*. Cichoric acid from witloof inhibit misfolding aggregation and fibrillation of hIAPP. International Journal of Biological Macromolecules. 2020; 148: 1272–1279.

[7] Peng Y, Sun Q, Park Y. The Bioactive Effects of Chicoric Acid As a Functional Food Ingredient. Journal of Medicinal Food. 2019; 22: 645–652.

[8] Lu W, Chen Z, Wen J. RhoA/ROCK signaling pathway and astrocytes in ischemic stroke. Metabolic Brain Disease. 2021; 36: 1101–1108.

[9] Wei X, Lou H, Zhou D, Jia Y, Li H, Huang Q, *et al*. TAGLN mediated stiffness-regulated ovarian cancer progression via RhoA/ROCK pathway. Journal of Experimental & Clinical Cancer Research: CR. 2021; 40: 292.

[10] Tsai YL, Chiu CC, Yi-Fu Chen J, Chan KC, Lin SD. Cytotoxic effects of Echinacea purpurea flower extracts and cichoric acid on human colon cancer cells through induction of apoptosis. Journal of Ethnopharmacology. 2012; 143: 914–919.

[11] Chakraborti S, Sarkar J, Chowdhury A, Chakraborti T. Role of ADP ribosylation factor6-Cytohesin1-PhospholipaseD signaling axis in U46619 induced activation of NADPH oxidase in pulmonary artery smooth muscle cell membrane. Archives of Biochemistry and Biophysics. 2017; 633: 1–14.

[12] Ding X, Jian T, Li J, Lv H, Tong B, Li J, *et al*. Chicoric Acid Ameliorates Nonalcoholic Fatty Liver Disease via the AMPK/Nrf2/NFκB Signaling Pathway and Restores Gut Microbiota in High-Fat-Diet-Fed Mice. Oxidative Medicine and Cellular Longevity. 2020; 2020: 9734560.

[13] Zhou R, Yang X, Li X, Qu Y, Huang Q, Sun X, *et al*. Recombinant CC16 inhibits NLRP3/caspase-1-induced pyroptosis through p38 MAPK and ERK signaling pathways in the brain of a neonatal rat model with sepsis. Journal of Neuroinflammation. 2019; 16: 239.

[14] Li J, Ma X, Chakravarti D, Shalapour S, DePinho RA. Genetic and biological hallmarks of colorectal cancer. Genes & Development. 2021; 35: 787–820.

[15] Biller LH, Schrag D. Diagnosis and Treatment of Metastatic Colorectal Cancer: A Review. JAMA. 2021; 325: 669–685.

[16] Díaz-Tasende J. Colorectal cancer screening and survival. Revista Espanola De Enfermedades Digestivas. 2018; 110: 681–683.

[17] Baidoun F, Elshiwy K, Elkeraie Y, Merjaneh Z, Khoudari G, Sarmini MT, *et al*. Colorectal Cancer Epidemiology: Recent Trends and Impact on Outcomes. Current Drug Targets. 2021; 22: 998–1009.

[18] Ma Z, Lou S, Jiang Z. PHLDA2 regulates EMT and autophagy in colorectal cancer via the PI3K/AKT signaling pathway. Aging. 2020; 12: 7985–8000.

[19] Sun X, Zhang X, Zhai H, Zhang D, Ma S. Chicoric acid (CA) induces autophagy in gastric cancer through promoting endoplasmic reticulum (ER) stress regulated by AMPK. Biomedicine & Pharmacotherapy Biomedecine & Pharmacotherapie. 2019; 118: 109144.

[20] Ko E, Kim D, Min DW, Kwon SH, Lee JY. Nrf2 regulates cell motility through RhoA-ROCK1 signalling in non-small-cell lung cancer cells. Scientific Reports. 2021; 11: 1247.

[21] Yu G, Wang Z, Zeng S, Liu S, Zhu C, Xu R, *et al*. Paeoniflorin Inhibits Hepatocyte Growth Factor-(HGF-) Induced Migration and Invasion and Actin Rearrangement via Suppression of c-Met-Mediated RhoA/ROCK Signaling in Glioblastoma. BioMed Research International. 2019; 2019: 9053295.

[22] Xu N, Liu F, Wu S, Ye M, Ge H, Zhang M, *et al*. CHD4 mediates proliferation and migration of non-small cell lung cancer via the RhoA/ROCK pathway by regulating PHF5A. BMC Cancer. 2020; 20: 262.

[23] Ghasemi A, Hashemy SI, Aghaei M, Panjehpour M. RhoA/ROCK pathway mediates leptin-induced uPA expression to promote cell invasion in ovarian cancer cells. Cellular Signalling. 2017; 32: 104–114.

[24] Yang Y, Li L, He H, Shi M, He L, Liang S, *et al*. Numb inhibits migration and promotes proliferation of colon cancer cells via RhoA/ROCK signaling pathway repression. Experimental Cell Research. 2022; 411: 113004.